

RESEARCH

Open Access



Application of copy number variation sequencing combined with whole exome sequencing in prenatal left–right asymmetry disorders

Yu Qin¹, Muon Senglong¹, Koksear Touch¹, Juan Xiao¹, Ruijie Fang¹, Qingling kang¹, Lei Fan¹, Shufang Li¹, Jing Liu¹, Jianli Wu¹, Yuanyuan Wu¹, Xinwei Shi¹, Haiyi Liu¹, Xun Gong¹, Xingguang Lin¹, Ling Feng¹, Suhua Chen^{1*}  and Wei Li^{1*}

Abstract

Background Left–right (LR) asymmetry disorders present a complex etiology, with genetic factors emerging as a primary contributor. This study aims to explore the genetic underpinnings of chromosomal variants and individual genes in fetuses afflicted with prenatal LR asymmetry disorder.

Methods Through a retrospective analysis conducted between 2020 and 2023 at Tongji Hospital, Huazhong University of Science and Technology, genetic outcomes of LR asymmetric disorder were scrutinized utilizing copy number variation sequencing (CNV-seq) and whole exome sequencing (WES) methodologies.

Results With a combination of CNV-seq and WES, 5 fetuses in 17 patients with LR asymmetry had chromosomal or genetic variants. CNV-seq revealed a 16p11.2 microdeletion syndrome in a situs inversus fetus presenting pathogenic and a 2q36.3 microduplication syndrome in a fetus with Heterotaxy presenting a variant of uncertain significance (VUS). WES identified NM_198075.4:c.755del in the LRR56 gene and NM_001454.4:c.865_868dup in the FOXJ1 gene in two situs inversus cases, along with two variants in DNAH5 in two other fetuses. Further bioinformatics scrutiny was conducted to assess the protein structure and function prediction of these variants, ultimately indicating their potential pathogenicity.

Conclusion The study highlights that fetuses with LR asymmetric disorders may have copy number variants, underscoring the significance of mutations in LRR56 and FOXJ1 in the development of LR asymmetry disorders.

Keywords Left–Right asymmetry disorder, Situs Inversus, Heterotaxy, Copy number variant sequencing, Whole exome sequencing

Background

The normal pattern of asymmetrical arrangement of visceral organs along the left–right axis of the body is a complex and coordinated developmental process in humans and other vertebrates [1]. Failure to establish normal organ asymmetry along the left–right axis can lead to disorders of asymmetry with left–right (LR) asymmetry disorders including Situs Inversus (SI) and Heterotaxy

*Correspondence:

Suhua Chen

tj_csh@163.com

Wei Li

topliwei@126.com

¹ Department of Obstetrics and Gynecology, Tongji Hospital, Tongji Medical College, Huazhong University of Science and Technology, Jiefang Avenue 1095, Wuhan, Hubei 430030, China



© The Author(s) 2025. **Open Access** This article is licensed under a Creative Commons Attribution-NonCommercial-NoDerivatives 4.0 International License, which permits any non-commercial use, sharing, distribution and reproduction in any medium or format, as long as you give appropriate credit to the original author(s) and the source, provide a link to the Creative Commons licence, and indicate if you modified the licensed material. You do not have permission under this licence to share adapted material derived from this article or parts of it. The images or other third party material in this article are included in the article's Creative Commons licence, unless indicated otherwise in a credit line to the material. If material is not included in the article's Creative Commons licence and your intended use is not permitted by statutory regulation or exceeds the permitted use, you will need to obtain permission directly from the copyright holder. To view a copy of this licence, visit <http://creativecommons.org/licenses/by-nc-nd/4.0/>.

(HTX) [2]. SI is characterized by a mirror-image distribution of the thoracic and abdominal viscera in a position opposite to the normal anatomical state, with a prevalence of approximately 1/25,000–1/8000 [3]. SI typically maintains organ coordination, leading to infrequent occurrences of combined organ structural malformations. Conversely, HTX is characterized by stochastic visceral localization, where at least one of the thoracic and abdominal organs is inverted, presenting an incidence of 1/10,000 in newborns [4]. HTX frequently coexists with organ malformations, with approximately 80% of affected patients experiencing complex congenital heart diseases (CHDs) that are associated with a grim prognosis [5].

LR asymmetry disorders encompass a genetically diverse array of conditions that are influenced by a combination of genetic, environmental, and developmental stochastic factors, leading to incomplete penetrance [6]. Genetic factors encompass chromosomal abnormalities, and gene mutations [7]. Copy number variants have been identified in approximately 13.5% to 30.15% of cases of LR asymmetry disorders [8–10]. Genetic variants are present in about 15.3–56% of LR asymmetry disorder cohort studies [11–13], demonstrating a spectrum of inheritance patterns including autosomal recessive (AR), autosomal dominant (AD), and X-linked modes [14]. Over 82 genetic defects have been documented in academic literature as linked to LR asymmetry disorders [15]. Currently, common clinical methods for detecting copy number variants include chromosome microarray (CMA) or CNV-seq techniques. Whole exome sequencing, a high-throughput technology that sequences all exons of an organism, has gained popularity in clinical studies of rare disorders. This method allows for rapid analysis of multiple gene sequences, leading to a more thorough genetic diagnosis [16, 17].

In this study, a cohort of 17 fetuses with LR asymmetry disorder was analyzed using CNV-seq and WES. Potential pathogenic genes and variants were identified and confirmed through Sanger sequencing, and their pathogenicity was investigated using protein structure prediction modeling. These efforts were undertaken to provide new insights into the genetic etiology of LR asymmetry disorders.

Methods

Information of participants

This was a retrospective study carried out at the Prenatal Diagnostic Center of Tongji Hospital, Tongji Medical College, Huazhong University of Science and Technology, a renowned prenatal diagnostic referral center in China, spanning from January 2020 to August 2023. The study examined 17 cases of fetuses with SI or HTX, with data collection encompassing a range of clinical parameters

including gestational age at diagnosis, fetal ultrasound findings, pregnancy outcome, as well as demographic information such as the age of the couple, pregnancy history, and relevant family medical history. Our study was approved by the Research Ethics Committee of Tongji Hospital (TJ-IRB202401031). Informed consent was obtained from all participants in the study.

Sample collection and processing

Amniotic fluid was obtained through ultrasound-guided amniocentesis during mid-gestation in 14 instances for prenatal diagnosis. Fetal tissue was collected following delivery of the fetus in 2 cases where termination of pregnancy was opted for, while umbilical cord blood was collected at the time of full-term delivery in 1 case. Fetal genomic DNA was extracted from the samples using a DNA extraction kit (Tian Gen, Beijing, China) and stored at -20 °C for future analysis.

Copy number variation sequencing

CNV-seq was performed as previously described [18]. Briefly, genomic DNA was extracted from fetal tissues using the DNeasy Blood and Tissue Kit (Qiagen GmbH, Hilden, Germany). The quality and concentration of DNA were assessed with a Qubit 2.0 fluorometer (Thermo Fisher Scientific, Waltham, MA, USA). Approximately 5 million sequencing reads per sample were aligned to the NCBI human reference genome (hg19/GRCh37) using the Burrows-Wheeler Aligner (BWA) and organized into 20-kb blocks with a 5-kb sliding window for enhanced CNV detection.

Validation of CNVs was conducted by cross-referencing public repositories such as DGV (<http://dgv.tcag.ca/dgv/app/home>), DECIPHER (<http://decipher.sanger.ac.uk/>), Online Mendelian Inheritance in Man (OMIM, <http://www.omim.org/>), and UCSC (<http://genome.ucsc.edu/>), followed by assessment under the 2019 American College of Medical Genetics and Genomics (ACMG) guidelines [19]. Upon identification of fetal CNVs deemed pathogenic or potentially pathogenic, it is advised to procure blood samples from both parents for verification.

Finally, we analyzed the enrichment of genes identified in copy number variations (CNVs) using the DAVID database (<https://david.ncifcrf.gov/>). Subsequently, we assessed the influence of these genes on patient-specific phenotypes through Phenolyzer (<https://phenolyzer.wglab.org/>).

Short tandem repeat (STR) analysis

DNA samples were procured from fetal tissue and maternal peripheral blood to detect maternal contamination. Employing the Microreader™ 21 Direct ID System kit,

we executed multiplex PCR amplification with five-color fluorescent labeling across 20 commonly utilized STR loci and one sex locus. The resultant amplified products underwent separation via capillary electrophoresis, with subsequent analysis predicated on the repeat counts and lengths associated with each STR locus. Finally, GeneMapper ID version 3.2 software was used to interpret the electrophoresis profiles and determine the repeat numbers at each STR locus.

Whole exome sequencing

DNA samples were enriched for exome sequencing using the Agilent SureSelect Human Exome Capture Probe (V6, Life Technologies). The libraries underwent sequencing to generate paired-end reads of 150 base pairs on the HiSeq XTen platform (Illumina, Inc.). BAM files were created through a series of analyses including single nucleotide polymorphism detection, repeat annotation, insertion-deletion realignment, and quality recalibration utilizing GATK and SAM tools. All identified variants were classified as pathogenic, likely pathogenic (LP), variant of unknown significance (VUS), likely benign, or benign based on the criteria outlined by the ACMG [20]. Sanger sequencing was employed for verification in cases where fetal likely pathogenic and pathogenic gene variants were identified. It is recommended that Sanger sequencing be conducted on blood samples obtained from both parents when fetal pathogenic or likely pathogenic variants are discovered.

Conservation analysis of mutated genes and mutation frequency analysis

The methodology for assessing species conservation entailed retrieving protein sequences linked to mutated human genes, and those from diverse species, from the National Center for Biotechnology Information (NCBI) database (<https://www.ncbi.nlm.nih.gov/>). Subsequently, the conservation of these protein sequences across different species was analyzed using the Clustal X software.

To analyze the frequencies of mutations in disease-causing genes within the population, data from the Thousand Genomes Project (1000G) (<https://www.internationalgenome.org/>), the Human Exome Database (ExAC) (<http://exac.broadinstitute.org/>), and the Genome Aggregation Database (gnomAD) (<https://gnomad.broadinstitute.org/>) were consulted as references.

Protein structure and function prediction of mutant genes

The methodology for predicting the protein structure of mutant genes involved utilizing the online SWISS-MODEL tool (<http://www.swissmodel.expasy.org>) to predict both wild-type and mutant protein structures,

followed by PyMOL software (version 1.7, Schrödinger, LLC, Portland, U.S.A.) to create visual representations.

Three methods were utilized to predict mutant gene function including Mutation Taster (<http://www.mutationtaster.org/>) [21], Polyphen-2 (<http://genetics.bwh.harvard.edu/pph2/>), and PROVEAN (<http://provean.jcvi.org/index.php>) [22].

Results

Basic information

As indicated in Table 1, ultrasonography of 17 pediatric patients revealed SI in 12 cases and HTX in 5 cases, with no reported history of consanguinity among the couples. Additionally, three cases had a history of stillbirth pregnancies, and one had a history of fetal intestinal exstrophy, but genetic testing was not performed for the fetus or the couple.

Results of copy number variation sequencing

In this investigation, 2 fetuses with abnormal CNVs were detected but were not further verified by other methods (Supplementary Information Fig. 1). Case 7, diagnosed with SI, exhibited a de novo pathogenic 0.56 Mb deletion at p11.2 of chromosome 16. After reviewing the ClinGen database, there is substantial evidence (Haploinsufficiency score: 3) that patients with a single dose deficiency in this region display the clinical phenotype of Chromosome 16p11.2 deletion syndrome, 593-KB (OMIM: 611,913), with a penetrance of approximately 46.8% [23–25]. Patients primarily exhibit developmental delays of varying severity, neurological abnormalities, scoliosis, or hemivertebrae deformities, with about 6% also presenting congenital heart disease, leading to a classification of this variant as pathogenic. Conversely, Case 14, diagnosed with HTX, displayed a chromosomally identified 1.06 Mb heterozygous duplication at q36.3 of chromosome 2. Multiple database resources were queried and no case information or population evidence associated with this fragment was found, leading to a classification of this variant as VUS. Notably, CNV testing was not conducted on the parents of the last affected fetus. As illustrated in Table 2, the CNVs above encompassed 50 genes, which underwent enrichment and analysis. These genes were enriched in pathways like PI3K-Akt signaling and cellular migration, which are essential for normal organ development and left–right asymmetry (Supplementary Information Fig. 2). In addition, we identified 20 genes with potential associations with the SI and HTX, as detailed in Supplementary Information Table 1.

Results of whole exome sequencing

The study revealed a detection rate of 11.8% (2/17) for core findings identified through Whole-exome sequencing

Table 1 Clinical information of 17 fetuses with LR asymmetry disorder

Case	Maternal age	Gestational age (week)	History of adverse pregnancy	LR asymmetry disorders	Heterotaxy signs	Abnormal ultrasound findings other than SI or HTX	Results of CNV-seq		Results of the WES		Outcome of pregnancy	Follow-up of live births
							Chromosomes	ACMG classification	Gene	ACMG classification		
1	25	24 ⁺³	/	SI	/	/	/	/	LRRCS6	P	TOP	/
2	26	23	/	SI	/	/	/	/	FOXJ1	LP	TOP	/
3	26	18	/	SI	/	VSD, SUA, Reversed a-wave in DV spectrum	/	/	/	/	TOP	/
4	29	23 ⁺²	/	SI	/	/	/	/	/	/	Live birth	Healthy
5	38	33 ⁺²	/	HTX	Stomach on the right	Slight thickening of the right ventricle of the heart	/	/	/	/	Live birth	Healthy
6	34	24 ⁺²	/	HTX	Stomach on the right; liver in a horizontal position; gallbladder in the midline	Interruption of inferior vena cava	/	/	/	/	Live birth	Healthy
7	34	40 ⁺¹	/	SI	/	/	Del 16p11.2p11.2	P	DNAH5 [#]	VUS	Live birth	Healthy
8	24	23 ⁺⁶	/	SI	/	/	/	/	/	/	Live birth	Healthy
9	32	19 ⁺⁴	Stillbirth 2 times	HTX	Dextrocardia	Abnormal development of the left hand	/	/	/	/	TOP	/
10	30	22	/	SI	/	AVSD, DORV	/	/	/	/	TOP	/
11	40	24 ⁺²	Stillbirth 1 time	HTX	Stomach on the right	AVSD, SA, Interruption of inferior vena cava, ARSA	/	/	/	/	TOP	/
12	32	18 ⁺³	/	SI	/	/	/	/	DNAH5 [#]	VUS	TOP	/
13	28	19 ⁺⁶	Fetal intestinal exstrophy 1 time	SI	/	/	/	/	/	/	Live birth	Healthy
14	37	15 ⁺³	Stillbirth 1 time	HTX	Stomach on the right; liver on the left side	SV, AVSD	Dup 2q36.3q36.3	VUS	/	/	TOP	/
15	26	23	/	SI	/	/	/	/	/	/	TOP	/
16	31	23 ⁺⁴	/	SI	/	/	/	/	/	/	Live birth	Healthy
17	35	22 ⁺⁵	/	SI	/	/	/	/	/	/	Live birth	Healthy

ARSA, Aberrant right subclavian artery, AVSD Atrio-ventricular septal defect, DORV Double outlet of the right ventricle, DV Ductus venosus, HTX Heterotaxy, LP Likely pathogenic, P Pathogenic, SA Single atrium, SI Situs inversus, SUA Single umbilical artery, SV Single ventricle, TOP Termination of pregnancy, VSD Ventricular Septal Defects
 #Compound heterozygote

Table 2 Localization of pathogenic or VUS CNVs and the genes they contain

Cases	Chromosome	Genomic coordinates	Type	Size (Mb)	Genes contained
7	16p11.2p11.2	29,640,000–30,200,000	Del	0.56	ALDOA, SPN, QPRT, RN7SKP127, C16orf54, ZG16, KIF22, MAZ, MVP-DT, PRRT2, PAGR1, MVP, CDIPT, CDIPTOSP, SEZ6L2, ASPHD1, KCTD13, KCTD13-DT, TMEM219, TAOK2, HIRIP3, INO80E, DOC2A, C16orf92, TLCD3B, PPP4C , TBX6 , YPEL3, YPEL3-DT, GDPD3, MAPK3, CORO1A, CORO1A-AS1, BOLA2B, SLX1A, SLX1A-SULT1A3, SULT1A3
14	2q36.3q36.3	226,540,000–227,600,000	Dup	1.06	MIR5702, IRS1, RHBDD1, COL4A4, COL4A3, MFF-DT, MFF, TM4SF20, SCYGR1, MIR5703, AGFG1, SCYGR9, SCYGR2

(WES) in fetuses or neonates exhibiting LR asymmetry disorders. As shown in Table 3, case 1 involved the identification of a definitive homozygous pathogenic variant in LRRC56, with both fetal parents found to be asymptomatic heterozygous carriers. In case 2, a likely pathogenic de novo heterozygous variant in FOXJ1 was discovered, both genes being linked to primary ciliary dyskinesia (PCD). Additionally, cases 7 and 12, both SI fetuses, were found to have two variants in the DNAH5 gene (Supplementary Information Table 2). These variants were classified as variants of uncertain significance (VUS) according to the guidelines of the ACMG due to limited evidence, based on single existing evidence. The remaining 12 fetuses tested negative for the variants mentioned above.

Protein structure prediction of the mutated gene and Sanger sequencing analysis

The fetus in Case 1 exhibited a homozygous c.755 base deletion in the LRRC56 gene, resulting in p.Val252GlyfsTer158 as illustrated in Figs. 1a and 2a. Figure 3a showed significant evolutionary conservation at residue 252 among various species. This genetic modification led to a disruption in the amino acid sequence, causing premature termination (1–408 aa) and subsequent structural abnormalities within the central region of the protein. As detailed in Table 3, it exhibited a frequency of 0.000006746 in the gnomAD. The mutation was validated by Sanger sequencing (Fig. 4a) and was inherited from asymptomatic heterozygous carrier parents to the

Table 3 Frequency of mutated genes in LRRC56 and FOXJ1 and prediction of mutated gene function

Gene symbol	LRRC56	FOXJ1
Gene’s nomenclature	Leucine rich repeat containing 56	Forkhead box J1
Variant location	chr11:551,261–551,261	chr17:76,137,750–76137750
Transcript	NM_198075.4:c.755del	NM_001454.4:c.865_868dup
Variant	NP_932341.1:p.(Val252GlyfsTer158)	NP_001445.2:p.(Ser290ThrfsTer13)
Zygoty	Homozygous	Heterozygous
Origins of Mutation	Parental	De-novo
Variant type	Frameshift insertion	Frameshift insertion
dbSNP	rs1424720789	-
Allelic frequencies	1000G ExAC gnomAD	- - -
Diseases	Primary ciliary dyskinesia type 39	Primary ciliary dyskinesia type 43
Inheritance patterns	autosomal recessive	autosomal dominant
ACMG classification	Pathogenic (PVS1 + PM2_Supporting + PM3_Supporting)	Likely pathogenic (PS2 + PM2)

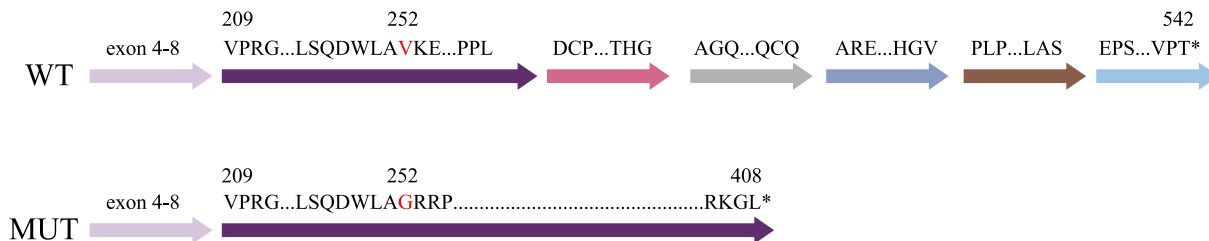
NM_198075.4(LRRC56):c.755del:

1. Strong pathogenic evidence PVS1: This variant causes a change in the open reading frame of the gene, leading to altered protein function
2. Supporting pathogenic evidence PM2_Supporting: This variant has not been found in the reference populations of the 1000 Genomes Project (1000G), the Chinese Genome Database, or the Exome Aggregation Consortium (ExAC). Its frequency in the Genome Aggregation Database (gnomAD) is 0.000001441
3. Supporting pathogenic evidence PM3_Supporting: The variant was detected in a homozygous state in the examined individual

NM_001454.4(FOXJ1):c.865_868dup:

1. Strong pathogenic evidence PS2: This variant is a de novo mutation identified through trio analysis in family samples
2. Moderate pathogenic evidence PM2: This variant has not been found in the Chinese Genome Database, the Exome Aggregation Consortium (ExAC), the 1000 Genomes Project (1000G), or the Genome Aggregation Database (gnomAD)

a. LRRC56



b. FOXJ1

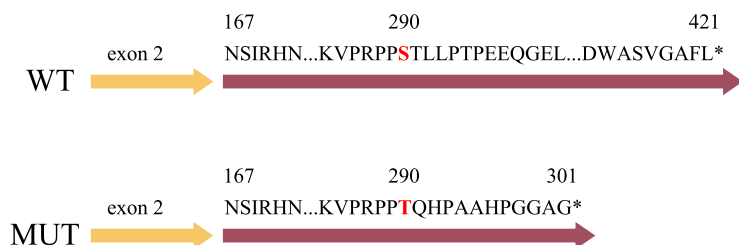


Fig. 1 Comparison of protein structure prediction maps before and after mutation of LRRC56 and FOXJ1. **a** The upper panel displays the predicted structure of the wild-type protein of LRRC56, consisting of 542 amino acids. Conversely, the lower panel demonstrates the impact of the deletion of the 755th base of the LRRC56 gene, resulting in a change from valine to glycine at the 252nd amino acid position of the encoded protein. Furthermore, the predicted structure of the mutant protein of LRRC56 indicates a code-shifting mutation at the mutant site, leading to early termination of the protein at 408 amino acids. **b** The upper panel depicts the anticipated structure of the wild-type FOXJ1 protein, comprising 421 amino acids. Conversely, the lower figure illustrates a substitution of serine to threonine at the 290th amino acid position following a duplication event at bases 865–868. Furthermore, the mutation of FOXJ1 leads to a frameshift mutation and premature termination of the protein at amino acid 301. Each exon is represented by distinct colored arrows

fetus. The designation of this variant as pathogenic is consistent with the guidelines established by the ACMG (PVS1 + PM2_Supporting + PM3_Supporting).

In Case 2, duplication of bases c.865–868 in the fetal FOXJ1 gene resulted in the p.Ser290ThrfsTer13 mutation, leading to premature termination (1–301 aa) and disruption of critical protein structures (Figs. 1b and 2b). Figure 3b showed significant evolutionary conservation at residue 290 among various species. Protein function prediction analyses using Polyphen-2 and PROVEAN indicated benign and potentially adaptive effects, respectively (Table 3). In addition, Sanger sequencing validation (Fig. 4b) confirmed the variant as a de novo heterozygous mutation, and it is designated as likely pathogenic according to ACMG guidelines (PS2 + PM2).

Pregnancy outcome and prognosis

This study reported 9 pregnancy terminations and 8 full-term deliveries. Two families with fetal pathogenic and likely pathogenic gene mutations chose to terminate pregnancies (Cases 1 and 2). In the first family, both parents carried a heterozygous pathogenic variant in an autosomal recessive gene, prompting our recommendation of Pre-implantation Genetic Testing (PGT) for a

future pregnancy. In the second family, we advised natural conception with prenatal diagnostics due to a de novo mutation (Case 2). In the full-term deliveries, a fetus with a pathogenic Copy Number Variant (CNV) coupled with a gene of VUS was delivered in June 2022 (Case 7). A neonatal ultrasound diagnosis confirmed SI, but no vital organ dysfunction was observed during follow-ups up to 2 years. The other five SI and two HTX cases tested negative for CNV-seq and Whole-Exome Sequencing (WES), with no vital organ dysfunction noted in postnatal evaluations.

Discussion

This retrospective cohort study aimed to assess the impact of genetic variations on fetal LR asymmetry. In the cohort, WES identified 2 fetuses with pathogenic or likely pathogenic genes, and 2 with VUS genes, and CNV-seq detected 1 microdeletion syndrome and 1 microduplication syndrome.

Some rare Copy Number Variants (CNVs) have been implicated in certain disorders related to LR asymmetry disorders, with many of these CNVs harboring key genes crucial for organ development pattern [9, 10, 26, 27]. In this study, case 7 exhibited a 16p11.2 deletion and had a

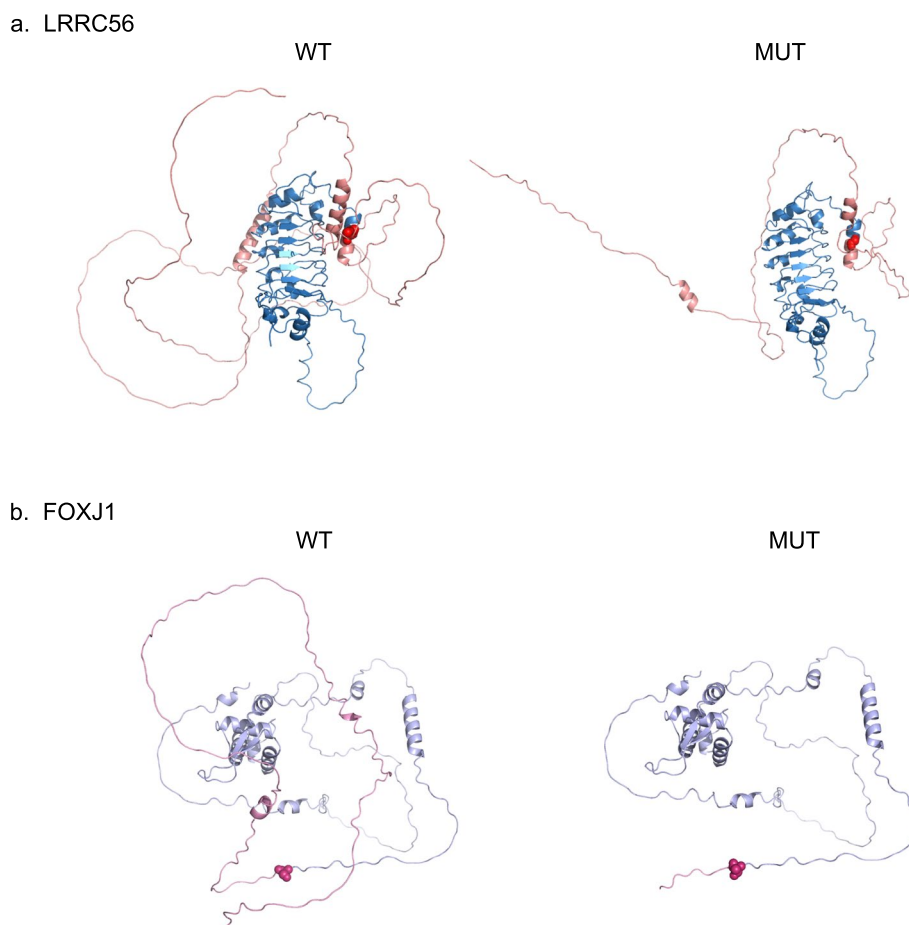


Fig. 2 Comparison of 3D protein structure prediction before and after LRRC56 and FOXJ1 mutations. **a** The left panel is the LRRC56 wild-type protein, which has its 252nd amino acid highlighted in a red sphere. The right panel shows the LRRC56 mutant protein, with the 252nd amino acid highlighted as a red sphere, and its protein structure is significantly smaller compared to the wild-type protein structural domain. **b** The left panel is the FOXJ1 wild-type protein, whose 290th amino acid is highlighted by a red sphere. On the right is the FOXJ1 mutant protein, whose 290th amino acid is highlighted by a red sphere and whose protein structure is significantly smaller compared to the wild-type protein structural domain

VUS variant at 2 loci in DNAH5, the latter was the primary diagnosis. Despite this finding, the parents opted to proceed with the pregnancy, and the child, monitored biannually post-birth, displayed no clinical signs of microdeletion syndrome by age two. Previous studies on LR asymmetry disorders identified 16p11.2 deletions that include critical LR development genes TBX6 and PPP4C [27]. Animal experiments have shown that Tbx6 plays a role in LR patterning in mouse embryos by influencing lymph node cilium and perinodal signaling [28], and Ppp4c is essential for dorsoventral patterning in zebrafish embryos through the regulation of BMP/SMAD signaling, while the MGI database indicates that Ppp4c knockout mice do not exhibit LR asymmetry disorder [29]. However, the connection between this chromosomal variant and visceral inversion remains unclear, requiring further investigation.

The variant gene LRRC56, located on 11p15.5, consists of 14 exons and encodes a 542 amino acid protein with a leucine-rich repeat domain. It is widely expressed in humans, particularly in the testis and pituitary, and is predominantly transcribed in ciliated cells of the lung [30, 31]. In algal, its homolog ODA8 is crucial for the dynamin complex's role in flagellar assembly [32]. Studies have showcased that LRRC56 is involved in motility and cilia maintenance through intraflagellar transport (IFT), which relies on kinesin-2, and mutations in this gene are linked to several human diseases affecting cilia [33].

As shown in Table 4, a study documented mutations in the LRRC56 gene across three families [33]. For instance, a girl in one family with an NM_198075.4:c.423+1G>A variant experienced visceral inversion and recurrent lung infections, leading to a diagnosis of primary ciliary dyskinesia (PCD) [34]. Another family reported both fetuses with the NM_198075.4:c.419 T>C

a. LRRC56

	242										252										262					
MUT	P	P	R	L	S	Q	D	W	L	A	G	R	R	P	S	R	R	A	T	A	F					
HUMAN	P	P	R	L	S	Q	D	W	L	A	V	K	E	A	I	K	K	G	N	G	-					
RAT	P	Q	K	L	S	Q	D	W	L	M	V	K	E	A	I	K	E	G	N	V	L					
MOUSE	P	Q	T	L	S	Q	D	W	L	M	V	K	E	A	I	K	E	G	S	V	L					
BOVINE	S	Q	K	L	D	Q	D	W	L	L	V	K	E	A	I	K	E	G	C	T	L					
PIG	S	R	K	L	D	Q	D	W	L	M	V	K	Q	A	I	K	K	G	S	V	L					

b. FOXJ1

	282										290										301					
MUT	V	A	K	V	P	R	P	P	T	Q	H	P	A	A	H	P	G	G	A	G	*					
HUMAN	V	A	K	V	P	R	P	P	S	T	L	L	P	T	P	E	E	Q	G	E	L					
RAT	V	A	K	V	L	R	P	P	S	T	L	L	L	T	Q	E	E	Q	G	E	L					
MOUSE	V	A	K	V	L	R	P	P	S	T	L	L	L	T	Q	E	E	Q	G	E	L					
BOVINE	V	A	K	V	P	R	P	P	S	T	L	L	L	T	Q	E	E	Q	G	E	L					
PIG	V	A	K	V	P	R	P	S	S	T	L	L	L	T	Q	E	E	Q	G	E	L					

Fig. 3 Conservation analysis of LRRC56 and FOXJ1 mutation sites. The upper panel indicates a high degree of conservation at amino acid position 252 of LRRC56, while the lower panel demonstrates a similar conservation pattern at amino acid position 290 of FOXJ1

variant, linked to visceral anomalies and congenital heart disease. A separate family had a compound heterozygote with NM_198075.4:c.760G>T and NM_198075.4:c.326+1G>A, presenting with chronic lung infections and otitis media. Additionally, a cohort study in Saudi Arabia found the NM_198075.4:c.494 T>C variant in a family with visceral inversion and respiratory issues [35, 36]. Notably, we found a deletion at base 755 in LRRC56 leading to a frameshift mutation, which had not been previously documented. This novel variant was analyzed for its potential pathogenic role, enhancing the genetic understanding of LR asymmetric disorders.

A distinct variant of the FOXJ1 gene at 17q25.1 was also identified, which consists of three exons encoding the forkhead transcription factor (HFH-4), crucial for motor ciliogenesis. HFH-4 is highly expressed in various tissues, including airway-ciliated cells and the vas deferens, and is essential for the development of epithelial cells with motile cilia, playing a key role in establishing LR asymmetry and facilitating mucociliary clearance [37]. Heterozygous mutations in FOXJ1 can disrupt motor cilia structure and impact cerebrospinal fluid dynamics, contributing to hydrocephalus [38].

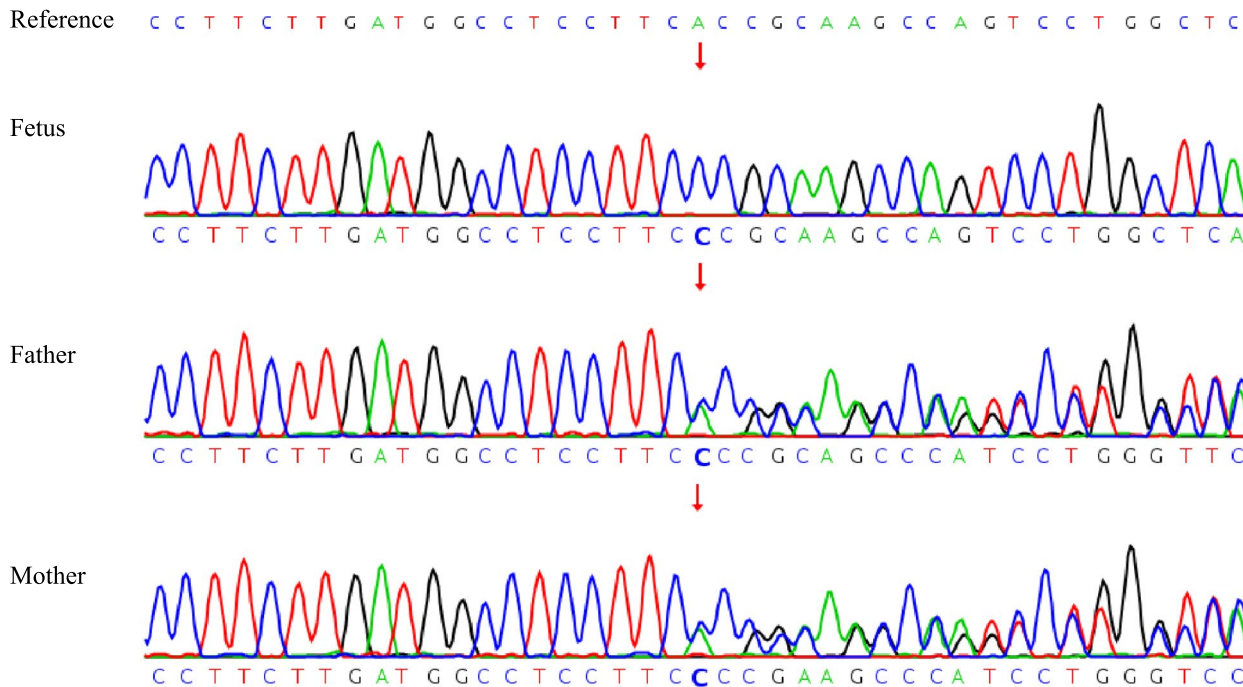
As shown in Table 5, a total of 14 patients with FOXJ1 mutations have been reported in the literature, 6 of whom exhibited situs inversus often alongside hydrocephalus

[39–43]. For instance, the NM_001454.4:c.784_799dup variant does not produce ectopic cilia or activate the ADGB promoter which is a downstream target of FOXJ1 associated with ciliary function, though it has been linked to complex congenital heart disease [44]. The fetuses in this study exhibited complete visceral inversion without cerebral edema, potentially reflecting the diverse phenotypes associated with various mutation loci. Notably, we identified a novel NM_001454.4:c.865_868dup variant in the FOXJ1 gene, which has not been previously reported.

Variants in the LRRC56 and FOXJ1 genes are associated with PCD, which is a genetically diverse group of disorders caused by abnormal ciliary motility, leading to various clinical presentations. This dysfunction manifests as compromised ciliary function in tissues and organs. Approximately 50% of PCD patients present with situs inversus (SI), and around 6% exhibit Heterotaxy (HTX), both of which pertain to left–right asymmetry disorders [45]. A cohort study of Chinese children with PCD identified DNAH11 as the most frequently mutated gene, with two variants in this study being previously unreported [46]. Therefore, this research expands the understanding of gene variants linked to PCD and left–right asymmetry in the Chinese population.

Our study involves a single-center investigation with a limited subject number, highlighting the need for future

a. mutation gene of LRRC56 in case 1 family



b. mutation gene of FOXJ1 in case 2 family

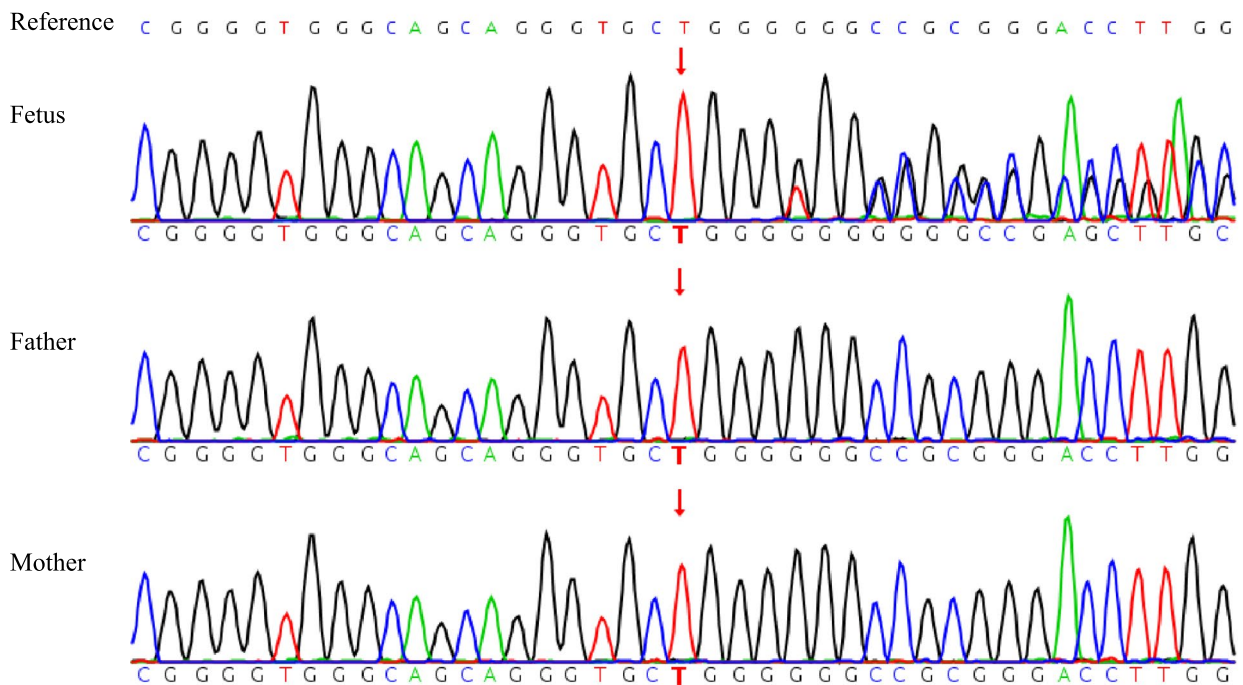


Fig. 4 Validation of LRRC56 and FOXJ1 variant sources by Sanger sequencing of family lines **a** mutation gene of LRRC56 in case 1 family **b** mutation gene of FOXJ1 in case 2 family

Table 4 Literature review of the variant loci of LRRC56

Case	Gender	Nationality	Age (year)	Situs inversus	CHD	Chronic inflammation of the respiratory system	LRRC56 transcript	Inheritance	Consanguineous marriages
1	Unknown	Chinese	0	+	-	-	NM_198075.4:c.755del	Paternal	-
2 [33, 34]	Female	British Pakistani	1.5	+	-	+	NM_198075.4:c.423 + 1G > A	Paternal	+
3 [33]	Unknown	Kuwaiti	0	+	+	-	NM_198075.4:c.419 T > C	Paternal	+
4 [33]	Male	British	27	+	-	+	NM_198075.4:c.760G > T and NM_198075.4:c.326 + 1G > A	de novo	-
5 [35, 36]	Male	Arabian	7	+	+	+	NM_198075.4:c.494 T > C	Unknown	+

^aThe two fetal represent complex congenital heart malformation characterized by double outlet right ventricle

Table 5 Literature review of the variant loci of FOXJ1

Case	Gender	Nationality	Age (years)	Situs inversus	CHD	Hydrocephalus	FOXJ1 transcript	Inheritance
1	Unknown	Chinese	0	+	-	-	NM_001454.4:c.865_868dup	de novo
2 [39]	Female	Chinese	4	+	-	+	NM_001454.4:c.734_735 ins20	de novo
3 [40]	Male	German	0	-	-	+	NM_001454.4:c.901G > T	de novo
4 [40]	Male	German	0	-	VSD	+	NM_001454.4:c.826C > T	de novo
5 [40]	Female	German	54	-	-	+	NM_001454.4:c.868_871dup	de novo
6 [40]	Female	British	0	-	-	+	NM_001454.4:c.967delG	de novo
7 [40]	Male	U.S	0	+	-	+	NM_001454.4:c.826C > T	de novo
8 [40]	Male	U.S	0	+	-	+	NM_001454.4:c.939delC	Unknown
9 [41]	Female	European	0	-	-	+	NM_001454.4:c.967delG	de novo
10 [41]	Male	European	0	-	-	+	NM_001454.4:c.826C > T	de novo
11 [41]	Male	European	0	-	-	+	NM_001454.4:c.287C > G	carrier mother
12 [42]	Female	German	0	+	ASD	+	NM_001454.4:c.945delC	de novo
13 [42]	Male	Irish	0	-	-	+	NM_001454.4:c.929_932delACTG	Unknown
14 [43]	Female	Japan	29	+	ESD	+	NM_001454.4:c.709delC	Unknown
15 [44]	Male	U.S	0	-	-	-	NM_001454.4:c.784_799dup	de novo

ASD Atrial septal defect, ESD Endocardial cushion defect, VSD Ventricular septal defect

collaborations to increase the sample size. With advancements in molecular genetics, such as single-cell sequencing, more genes related to visceral left–right axis development may be discovered, enhancing our comprehension of the molecular mechanisms underlying visceral inversion [47].

Conclusions

This is a retrospective analysis of a prenatal cohort with Situs Inversus and Heterotaxy. CNV-seq detected 16p11.2 microdeletion syndrome and 2q36.3 microduplication syndrome, while WES identified pathogenic and likely pathogenic de novo mutations in the LRRC56 and FOXJ1 genes, providing new genetic insights into LR asymmetry disorders.

Supplementary Information

The online version contains supplementary material available at <https://doi.org/10.1186/s12864-025-11277-7>.

Supplementary Material 1.

Acknowledgements

We would like to thank all individuals who participated in the screening program. We extend our gratitude to Berry Genomics Corporation (Beijing, China) for their expert technical assistance and data analysis. Special thanks to the following individuals: Qisen Qiao, Yang Bai, Xiang Wang, and Zhixian Zhao from Berry Genomics Corporation, Beijing 102200, China; and Yuanyuan Zhu from Becreative Lab Co. Ltd, Beijing, China. We also thank Professor Hongyun Liu from Tongji Hospital, Huazhong University of Science and Technology, for her guidance on our ultrasound results.

Authors' contributions

SC and WL participated in and designed the study. YQ, MS, KT, JX, RF, QK, LF, SL, JL, JW, YW, XS, HL, XG, XL, and LF collected medical records and interpreted data. YQ completed the data organization as well as drafted the manuscript. All authors read and approved the final version of the manuscript.

Funding

This work was supported by the Natural Science Foundation of Hubei Province (2024AFB1019).

Data availability

The CNV-seq data and WES data reported in this paper have been deposited in the Genome Sequence Archive (Genomics, Proteomics & Bioinformatics

2021) in National Genomics Data Center (Nucleic Acids Res 2022), China National Center for Bioinformation / Beijing Institute of Genomics, Chinese Academy of Sciences that are publicly accessible at <https://ngdc.cncb.ac.cn/gsa-human>. The accession number for the CNV-seq data is GSA-Human: HRA010120, and the accession number for the WES data is GSA-Human: HRA010118 [48, 49]. As Cases 2–5 in this study are unwilling to disclose their raw WES data, the datasets are available from the corresponding author upon reasonable request if needed.

Declarations

Ethics approval and consent to participate

The studies involving human participants were reviewed and approved by the guidance of the Ethics Committee of Tongji Hospital, Huazhong University of Science and Technology (TJ-IRB202401031). The patients provided their written informed consent to participate in this study. This study adheres to the principles outlined in the Helsinki Declaration.

Consent for publication

All authors read and approved the final manuscript. All patients have given their informed consent for their data and information to be published.

Competing interests

The authors declare no competing interests.

Received: 6 July 2024 Accepted: 22 January 2025

Published online: 28 January 2025

References

- Sutherland MJ, Ware SM. Disorders of left-right asymmetry: heterotaxy and situs inversus. *Am J Med Genet C Semin Med Genet.* 2009;151c:307–17. <https://doi.org/10.1002/ajmg.c.30228>.
- Deng H, Xia H, Deng S. Genetic basis of human left-right asymmetry disorders. *Expert Rev Mol Med.* 2015;16:e19. <https://doi.org/10.1017/erm.2014.22>.
- Chen W, Zhang Y, Shen L, Zhu J, Cai K, Lu Z, Zeng W, Zhao J, Zhou X. Biallelic DNAH9 mutations are identified in Chinese patients with defective left-right patterning and cilia-related complex congenital heart disease. *Hum Genet.* 2022;141:1339–53. <https://doi.org/10.1007/s00439-021-02426-5>.
- Lin AE, Ticho BS, Houde K, Westgate MN, Holmes LB. Heterotaxy: associated conditions and hospital-based prevalence in newborns. *Genet Med.* 2000;2:157–72. <https://doi.org/10.1097/00125817-200005000-00002>.
- Peeters H, Devriendt K. Human laterality disorders. *Eur J Med Genet.* 2006;49:349–62. <https://doi.org/10.1016/j.ejmg.2005.12.003>.
- Xia H, Huang X, Deng S, Xu H, Yang Y, Liu X, Yuan L, Deng H. DNAH11 compound heterozygous variants cause heterotaxy and congenital heart disease. *PLoS ONE.* 2021;16:e0252786. <https://doi.org/10.1371/journal.pone.0252786>.
- Yuan L, Yu X, Xiao H, Deng S, Xia H, Xu H, Yang Y, Deng H. Identification of novel compound heterozygous variants in the DNAH1 gene of a Chinese family with left-right asymmetry disorder. *Front Mol Biosci.* 2023;10:1190162. <https://doi.org/10.3389/fmolb.2023.1190162>.
- Liu C, Cao R, Xu Y, Li T, Li F, Chen S, Xu R, Sun K. Rare copy number variants analysis identifies novel candidate genes in heterotaxy syndrome patients with congenital heart defects. *Genome Med.* 2018;10:40. <https://doi.org/10.1186/s13073-018-0549-y>.
- Cowan JR, Tariq M, Shaw C, Rao M, Belmont JW, Lalani SR, Smolarek TA, Ware SM. Copy number variation as a genetic basis for heterotaxy and heterotaxy-spectrum congenital heart defects. *Philos Trans R Soc Lond B Biol Sci.* 2016;371. <https://doi.org/10.1098/rstb.2015.0406>.
- Fakhro KA, Choi M, Ware SM, Belmont JW, Towbin JA, Lifton RP, Khokha MK, Brueckner M. Rare copy number variations in congenital heart disease patients identify unique genes in left-right patterning. *Proc Natl Acad Sci U S A.* 2011;108:2915–20. <https://doi.org/10.1073/pnas.1019645108>.
- Bolkier Y, Barel O, Marek-Yagel D, Atias-Varon D, Kagan M, Vardi A, Mishali D, Katz U, Salem Y, Tirosh-Wagner T, et al. Whole-exome sequencing reveals a monogenic cause in 56% of individuals with laterality disorders and associated congenital heart defects. *J Med Genet.* 2022;59:691–6. <https://doi.org/10.1136/jmedgenet-2021-107775>.
- Yi T, Sun H, Fu Y, Hao X, Sun L, Zhang Y, Han J, Gu X, Liu X, Guo Y, et al. Genetic and clinical features of heterotaxy in a prenatal cohort. *Front Genet.* 2022;13:818241. <https://doi.org/10.3389/fgene.2022.818241>.
- Sun H, Yi T, Hao X, Yan H, Wang J, Li Q, Gu X, Zhou X, Wang S, Wang X, et al. Contribution of single-gene defects to congenital cardiac left-sided lesions in the prenatal setting. *Ultrasound Obstet Gynecol.* 2020;56:225–32. <https://doi.org/10.1002/uog.21883>.
- Zhu L, Belmont JW, Ware SM. Genetics of human heterotaxias. *Eur J Hum Genet.* 2006;14:17–25. <https://doi.org/10.1038/sj.ejhg.5201506>.
- Yu X, Yuan L, Deng S, Xia H, Tu X, Deng X, Huang X, Cao X, Deng H. Identification of DNAH17 variants in han-chinese patients with left-right asymmetry disorders. *Front Genet.* 2022;13:862292. <https://doi.org/10.3389/fgene.2022.862292>.
- Petrovski S, Aggarwal V, Giordano JL, Stosic M, Wou K, Bier L, Spiegel E, Brennan K, Stong N, Jobanputra V, et al. Whole-exome sequencing in the evaluation of fetal structural anomalies: a prospective cohort study. *Lancet (London, England).* 2019;393:758–67. [https://doi.org/10.1016/s0140-6736\(18\)32042-7](https://doi.org/10.1016/s0140-6736(18)32042-7).
- Bomba L, Walter K, Guo Q, Surendran P, Kundu K, Nongmaithem S, Karim MA, Stewart ID, Langenberg C, Danesh J, et al. Whole-exome sequencing identifies rare genetic variants associated with human plasma metabolites. *Am J Hum Genet.* 2022;109:1038–54. <https://doi.org/10.1016/j.ajhg.2022.04.009>.
- Qin Y, Touch K, Sha M, Sun Y, Zhang S, Wu J, Wu Y, Feng L, Chen S, Xiao J. The chromosomal characteristics of spontaneous abortion and its potential associated copy number variants and genes. *J Assist Reprod Genet.* 2024. <https://doi.org/10.1007/s10815-024-03119-4>.
- Riggs ER, Andersen EF, Cherry AM, Kantarci S, Kearney H, Patel A, Raca G, Ritter DI, South ST, Thorland EC, et al. Technical standards for the interpretation and reporting of constitutional copy-number variants: a joint consensus recommendation of the American College of Medical Genetics and Genomics (ACMG) and the Clinical Genome Resource (ClinGen). *Genet Med.* 2020;22:245–57. <https://doi.org/10.1038/s41436-019-0686-8>.
- Richards S, Aziz N, Bale S, Bick D, Das S, Gastier-Foster J, Grody WW, Hegde M, Lyon E, Spector E, et al. Standards and guidelines for the interpretation of sequence variants: a joint consensus recommendation of the American College of Medical Genetics and Genomics and the Association for Molecular Pathology. *Genet Med.* 2015;17:405–24. <https://doi.org/10.1038/gim.2015.30>.
- Schwarz JM, Cooper DN, Schuelke M, Seelow D. MutationTaster2: mutation prediction for the deep-sequencing age. *Nat Methods.* 2014;11:361–2. <https://doi.org/10.1038/nmeth.2890>.
- Won SY, Kim YC, Jeong BH. Elevated E200K Somatic Mutation of the Prion Protein Gene (PRNP) in the Brain Tissues of Patients with Sporadic Creutzfeldt-Jakob Disease (CJD). *Int J Mol Sci.* 2023;24. <https://doi.org/10.3390/ijms241914831>.
- Rein B, Yan Z. 16p11.2 Copy Number Variations and Neurodevelopmental Disorders. *Trends Neurosci.* 2020;43:886–901. <https://doi.org/10.1016/j.tins.2020.09.001>.
- Liu L, Wang J, Liu X, Wang J, Chen L, Zhu H, Mai J, Hu T, Liu S. Prenatal prevalence and postnatal manifestations of 16p11.2 deletions: A new insights into neurodevelopmental disorders based on clinical investigations combined with multi-omics analysis. *Clin Chim Acta.* 2024;552:117671. <https://doi.org/10.1016/j.cca.2023.117671>.
- Rosenfeld JA, Coe BP, Eichler EE, Cuckle H, Shaffer LG. Estimates of penetrance for recurrent pathogenic copy-number variations. *Genet Med.* 2013;15:478–81. <https://doi.org/10.1038/gim.2012.164>.
- Cowan J, Tariq M, Ware SM. Genetic and functional analyses of ZIC3 variants in congenital heart disease. *Hum Mutat.* 2014;35:66–75. <https://doi.org/10.1002/humu.22457>.
- Hagen EM, Sicko RJ, Kay DM, Rigler SL, Dimopoulos A, Ahmad S, Doleman MH, Fan R, Romitti PA, Browne ML, et al. Copy-number variant analysis of classic heterotaxy highlights the importance of body patterning pathways. *Hum Genet.* 2016;135:1355–64. <https://doi.org/10.1007/s00439-016-1727-x>.
- Hadjantonakis AK, Pisano E, Papaioannou VE. Tbx6 regulates left/right patterning in mouse embryos through effects on nodal cilia and

- perinodal signaling. *PLoS One*. 2008;3:e2511. <https://doi.org/10.1371/journal.pone.0002511>.
29. Jia S, Dai F, Wu D, Lin X, Xing C, Xue Y, Wang Y, Xiao M, Wu W, Feng XH, et al. Protein phosphatase 4 cooperates with Smads to promote BMP signaling in dorsoventral patterning of zebrafish embryos. *Dev Cell*. 2012;22:1065–78. <https://doi.org/10.1016/j.devcel.2012.03.001>.
 30. Uhlén M, Fagerberg L, Hallström BM, Lindskog C, Oksvold P, Mardinoglu A, Sivertsson Å, Kampf C, Sjöstedt E, Asplund A, et al. Proteomics. Tissue-based map of the human proteome. *Science*. 2015;347:1260419. <https://doi.org/10.1126/science.1260419>.
 31. Treutlein B, Brownfield DG, Wu AR, Neff NF, Mantalas GL, Espinoza FH, Desai TJ, Krasnow MA, Quake SR. Reconstructing lineage hierarchies of the distal lung epithelium using single-cell RNA-seq. *Nature*. 2014;509:371–5. <https://doi.org/10.1038/nature13173>.
 32. Desai PB, Freshour JR, Mitchell DR. Chlamydomonas axonemal dynein assembly locus ODA8 encodes a conserved flagellar protein needed for cytoplasmic maturation of outer dynein arm complexes. *Cytoskeleton (Hoboken)*. 2015;72:16–28. <https://doi.org/10.1002/cm.21206>.
 33. Bonnefoy S, Watson CM, Kernohan KD, Lemos M, Hutchinson S, Poulter JA, Crinnion LA, Berry I, Simmonds J, Vasudevan P, et al. Biallelic mutations in LRRC56, encoding a protein associated with intraflagellar transport, cause mucociliary clearance and laterality defects. *Am J Hum Genet*. 2018;103:727–39. <https://doi.org/10.1016/j.ajhg.2018.10.003>.
 34. Lucas JS, Barbato A, Collins SA, Goutaki M, Behan L, Caudri D, Dell S, Eber E, Escudier E, Hirst RA, et al. European Respiratory Society guidelines for the diagnosis of primary ciliary dyskinesia. *Eur Respir J*. 2017;49. <https://doi.org/10.1183/13993003.01090-2016>
 35. Asseri AA, Shati AA, Asiri IA, Aldosari RH, Al-Amri HA, Alshahrani M, Al-Asmari BG, Alalkami H. Clinical and Genetic Characterization of Patients with Primary Ciliary Dyskinesia in Southwest Saudi Arabia: A Cross Sectional Study. *Children (Basel)*. 2023;10. <https://doi.org/10.3390/children10101684>
 36. Alasmari BG, Saeed M, Alomari MA, Alsumaili M, Tahir AM. Primary Ciliary Dyskinesia: Phenotype Resulting From a Novel Variant of LRRC56 Gene. *Cureus*. 2022;14:e28472. <https://doi.org/10.7759/cureus.28472>.
 37. Blatt EN, Yan XH, Wuerffel MK, Hamilos DL, Brody SL. Forkhead transcription factor HFH-4 expression is temporally related to ciliogenesis. *Am J Respir Cell Mol Biol*. 1999;21:168–76. <https://doi.org/10.1165/ajrcmb.21.2.3691>.
 38. Hou CC, Li D, Berry BC, Zheng S, Carroll RS, Johnson MD, Yang HW. Heterozygous FOXJ1 Mutations Cause Incomplete Ependymal Cell Differentiation and Communicating Hydrocephalus. *Cell Mol Neurobiol*. 2023;43:4103–16. <https://doi.org/10.1007/s10571-023-01398-6>.
 39. Gao S, Zhang Q, Feng B, Gu S, Li Z, Sun L, Yao RE, Yu T, Ding Y, Wang X. A novel heterozygous variant of FOXJ1 in a Chinese female with primary ciliary dyskinesia and hydrocephalus: A case report and literature review. *Mol Genet Genomic Med*. 2023;11:e2235. <https://doi.org/10.1002/mgg3.2235>.
 40. Wallmeier J, Frank D, Shoemark A, Nöthe-Menchen T, Cindric S, Olbrich H, Loges NT, Aprea I, Dougherty GW, Pennekamp P, et al. De Novo Mutations in FOXJ1 Result in a Motile Ciliopathy with Hydrocephalus and Randomization of Left/Right Body Asymmetry. *Am J Hum Genet*. 2019;105:1030–9. <https://doi.org/10.1016/j.ajhg.2019.09.022>.
 41. Jin SC, Dong W, Kundishora AJ, Panchagnula S, Moreno-De-Luca A, Furey CG, Allocco AA, Walker RL, Nelson-Williams C, Smith H, et al. Exome sequencing implicates genetic disruption of prenatal neuro-gliogenesis in sporadic congenital hydrocephalus. *Nat Med*. 2020;26:1754–65. <https://doi.org/10.1038/s41591-020-1090-2>.
 42. Shapiro AJ, Kaspary K, Daniels MLA, Stonebraker JR, Nguyen VH, Joyal L, Knowles MR, Zariwala MA. Autosomal dominant variants in FOXJ1 causing primary ciliary dyskinesia in two patients with obstructive hydrocephalus. *Mol Genet Genomic Med*. 2021;9:e1726. <https://doi.org/10.1002/mgg3.1726>.
 43. Ito M, Morimoto K, Ohfuji T, Miyabayashi A, Wakabayashi K, Yamada H, Hijikata M, Keicho N. FOXJ1 Variants Causing Primary Ciliary Dyskinesia with Hydrocephalus: A Case Report from Japan. *Intern Med*. 2023. <https://doi.org/10.2169/internalmedicine.2565-23>.
 44. Padua MB, Helm BM, Wells JR, Smith AM, Bellchambers HM, Sridhar A, Ware SM. Congenital heart defects caused by FOXJ1. *Hum Mol Genet*. 2023;32:2335–46. <https://doi.org/10.1093/hmg/ddad065>.
 45. Knowles MR, Daniels LA, Davis SD, Zariwala MA, Leigh MW. Primary ciliary dyskinesia. Recent advances in diagnostics, genetics, and characterization of clinical disease. *Am J Respir Crit Care Med*. 2013;188:913–22. <https://doi.org/10.1164/rccm.201301-0059CI>.
 46. Guan Y, Yang H, Yao X, Xu H, Liu H, Tang X, Hao C, Zhang X, Zhao S, Ge W, et al. Clinical and genetic spectrum of children with primary ciliary dyskinesia in China. *Chest*. 2021;159:1768–81. <https://doi.org/10.1016/j.chest.2021.02.006>.
 47. Bellchambers HM, Phatak AR, Nenni MJ, Padua MB, Gao H, Liu Y, Ware SM. Single cell RNA analysis of the left-right organizer transcriptome reveals potential novel heterotaxy genes. *Sci Rep*. 2023;13:10688. <https://doi.org/10.1038/s41598-023-36862-2>.
 48. Database Resources of the National Genomics Data Center. China National Center for Bioinformatics in 2022. *Nucleic Acids Res*. 2022;50:D27–d38. <https://doi.org/10.1093/nar/gkab951>.
 49. Chen T, Chen X, Zhang S, Zhu J, Tang B, Wang A, Dong L, Zhang Z, Yu C, Sun Y, et al. The genome sequence archive family: toward explosive data growth and diverse data types. *Genomics Proteomics Bioinformatics*. 2021;19:578–83. <https://doi.org/10.1016/j.gpb.2021.08.001>.

Publisher's Note

Springer Nature remains neutral with regard to jurisdictional claims in published maps and institutional affiliations.